THE JOURNAL OF BIOLOGICAL CHEMISTRY VOL. 286, NO. 28, pp. 25187–25200, July 15, 2011

Protein Kinase C Promotes *N*-Methyl-D-aspartate (NMDA) Receptor Trafficking by Indirectly Triggering Calcium/Calmodulin-dependent Protein Kinase II (CaMKII) Autophosphorylation*[S]

Received for publication, October 8, 2010, and in revised form, April 14, 2011 Published, JBC Papers in Press, May 23, 2011, DOI 10.1074/jbc.M110.192708

Jing-Zhi Yan[‡§1], Zhuo Xu[‡§1], Si-Qiang Ren[‡§1], Bin Hu[‡§], Wen Yao[‡§], Shan-Hui Wang[‡§], Su-Yi Liu[‡§], and Wei Lu[‡§¶‖2]

From the [‡]Department of Neurobiology, [§]Key Laboratory for Neurodegenerative Disease of Jiangsu Province, [¶]Laboratory of Reproductive Medicine, and [‖]Key Laboratory for Human Functional Genomics of Jiangsu Province, Nanjing Medical University, Nanjing, Jiangsu Province 210029, China

Regulation of neuronal NMDA receptor (NMDAR) is critical in synaptic transmission and plasticity. Protein kinase C (PKC) promotes NMDAR trafficking to the cell surface via interaction with NMDAR-associated proteins (NAPs). Little is known, however, about the NAPs that are critical to PKC-induced NMDAR trafficking. Here, we showed that calcium/calmodulin-dependent protein kinase II (CaMKII) could be a NAP that mediates the potentiation of NMDAR trafficking by PKC. PKC activation promoted the level of autophosphorylated CaMKII and increased association with NMDARs, accompanied by functional NMDAR insertion, at postsynaptic sites. This potentiation, along with PKC-induced long term potentiation of the AMPA receptor-mediated response, was abolished by CaMKII antagonist or by disturbing the interaction between CaMKII and NR2A or NR2B. Further mutual occlusion experiments demonstrated that PKC and CaMKII share a common signaling pathway in the potentiation of NMDAR trafficking and long-term potentiation (LTP) induction. Our results revealed that PKC promotes NMDA receptor trafficking and induces synaptic plasticity through indirectly triggering CaMKII autophosphorylation and subsequent increased association with NMDARs.

The NMDA receptor (NMDAR)[3] plays a critical role in neural development, learning and memory, sensory perception, and synaptic plasticity (1, 2). Therefore, regulation of neuronal NMDARs is of great importance to synaptic transmission. PKC increases the NMDA channel opening rate and delivers new NMDARs to the plasma membrane through regulated exocytosis (3, 4). This potentiation of NMDAR trafficking is not due to phosphorylation of the NMDAR by PKC (5), suggesting that PKC indirectly exerts its effect through interaction with NMDAR-associated signaling and/or trafficking protein(s) (3, 4). Very recently, two elegant studies revealed that a SNARE protein, either SNAP-23 or SNAP-25, is such an NMDAR-associated trafficking protein that is critical to the promotion of NMDAR trafficking by PKC (6, 7). The PKC-dependent activation of the Src family of non-receptor protein kinases enhances NMDAR function mainly through increasing NMDAR channel gating (3, 8–11). It is still uncertain, however, whether an NMDAR-associated signaling protein that interacts with PKC displays a similar enhancing effect in NMDAR trafficking.

Numerous studies performed as early as the late 1980s support the idea of functional and positive cross-talk between CaMKII and PKC (12–15). One speculation based on these findings is that PKC and CaMKII act in series and share, at least partially, a common pathway by convergence in regulating certain common substrates. Interestingly, NMDAR could be such a common molecular target. Both PKC and CaMKII have phosphorylation sites on NMDAR. CaMKII is associated with both NR2A and NR2B NMDAR subunits (16–18). PKC potentiates NMDAR gating and in turn enhances Ca^{2+} influx and intracellular Ca^{2+}/camodulin, which could trigger CaMKII autophosphorylation and increase association with NR2A and NR2B subunits (16, 18).

Alterations in the synaptic NMDAR number and/or subunit composition caused by regulated NMDAR trafficking may contribute to the expression of LTP of NMDAR-mediated synaptic responses (19–21). However, the role of regulated NMDAR trafficking in the production of AMPAR-mediated synaptic plasticity is still uncertain. Taking into consideration that the synaptic trafficking of NMDARs is tightly regulated and has subunit-specific rules (22–24) and that the NMDAR NR2 subunit composition controls synaptic plasticity by regulating binding to CaMKII (25), it is of interest to determine whether PKC promotes NMDAR trafficking by regulating the association between CaMKII and NR2 subunits. Our present results revealed that CaMKII is indirectly activated by PKC and plays a critical role in PKC-induced potentiation of NMDAR postsyn-

* This work was supported by the National Natural Science Foundation of China (Grants 31025011 and 30970934), the Major State Basic Research Program of China (Grant 2010CB912002), and the Education Department of Jiangsu Province (Grant 08KJA180004) (all to W. L.).

[S] The on-line version of this article (available at http://www.jbc.org) contains supplemental Figs. 1–8.

[1] These authors contributed equally to this work.

[2] To whom correspondence should be addressed: Dept. of Neurobiology, Nanjing Medical University, Nanjing, Jiangsu Province 210029, China. Tel.: 86-25-86862822; Fax: 86-25-86862822; E-mail: lu@njmu.edu.cn.

[3] The abbreviations used are: NMDAR, NMDA receptor; CaMKII, calcium/calmodulin-dependent protein kinase II; NAP, NMDAR-associated protein; LTP, long-term potentiation; AMPAR, AMPA receptor; ACSF, artificial cerebrospinal fluid; EPSC, excitatory postsynaptic current; NMDA EPSCs, NMDAR-mediated EPSCs; PMA, phorbol 12-myristate 13-acetate; Myr, myristoylated; AIP, autocamtide-2-inhibitory peptide; PSD, postsynaptic density; CaM, calmodulin; p-CaMKII, phosphorylated CaMKII; TRITC, tetramethylrhodamine isothiocyanate; ANOVA, analysis of variance; LSD, least significant difference; IP, immunoprecipitation; TeTx, tetanus toxin.

aptic targeting. The increased association between CaMKII and NR2 subunits is critical for NMDAR trafficking and the accompanied synaptic plasticity produced by PKC.

EXPERIMENTAL PROCEDURES

Hippocampal Slice Preparation—Male Sprague-Dawley rats, 18–21 days old, were anesthetized with ethyl ether and decapitated. The entire hippocampus was removed. Coronal slices (350 μm) were cut on a vibrating blade microtome while in ice-cold artificial cerebrospinal fluid (ACSF) containing 126 mM NaCl, 2.5 mM KCl, 1 mM $MgCl_2$, 1 mM $CaCl_2$, 1.25 mM KH_2PO_4, 26 mM $NaHCO_3$, and 20 mM glucose (pH was adjusted to 7.4). ACSF was bubbled continuously with 95% O_2 and 5% CO_2. Fresh slices were incubated in a chamber with carbogenated ACSF and allowed to recover at 34 °C for at least 1.5 h before transfer to a recording chamber.

Electrophysiological Studies—Conventional whole-cell recordings were made with patch pipettes containing 132.5 mM cesium gluconate, 17.5 mM CsCl, 2 mM $MgCl_2$, 0.5 mM EGTA, 10 mM HEPES, 4 mM ATP, and 5 mM QX-314 with the pH adjusted to 7.2 by CsOH. Hippocampal slices were perfused with 34 °C ACSF bubbled continuously with 95% O_2 and 5% CO_2. Synaptic responses were evoked at 0.05 Hz. AMPAR-mediated excitatory postsynaptic currents (EPSCs) were recorded in ACSF perfusion medium containing bicuculline methiodide (10 μM) to block $GABA_A$ receptor-mediated inhibitory synaptic currents, whereas NMDAR-mediated EPSCs were recorded in ACSF perfusion medium containing both bicuculline methiodide (10 μM) and 2,3-dihydroxy-6-nitro-7-sulfamoyl-benzo[f]quinoxaline-2,3-dione (NBQX, 10 μM), and recorded cells were held at +40 mV. CA1 neurons were viewed under upright microscopy (Eclipse E600-FN, Nomasky, Nikon Corp., Tokyo, Japan) and recorded with an Axopatch-200B amplifier (Molecular Devices, Palo Alto, CA). Data were low pass-filtered at 2 kHz and acquired at 5–10 kHz. Recordings from each neuron lasted at least 40–80 min. The series resistance in these recordings varied between 4 and 6 megaohms. The series resistance was always monitored during recording to detect resealing of the ruptured membrane, which causes changes in both the kinetics and amplitude of the EPSCs. Cells in which the series resistance or capacitance deviated by >20% from initial values were excluded from analysis. Also, cells with series resistance >20 megaohms at any time during the recording were excluded. Data were collected with pClamp9.2 software and analyzed using Clampfit9.2 (Molecular Devices).

Subcellular Fractionation—Subcellular fractionation of hippocampal tissue was performed as described previously (12). Hippocampal slices were prepared as described above. Slices were then incubated in ACSF at 30 °C (95% O_2 and 5% CO_2) for 30 min. After the incubation period, slices were incubated for 15 min in the presence of phorbol 12-myristate 13-acetate (PMA; 0.5 μM) following preincubation with Tat-NR2A (0.5 μM), Tat-NR2B (0.5 μM), or myristoylated-AIP (Myr-AIP; 1 μM) for 20 min. After washing three times with fresh ACSF, slices were incubated for 10–15 min. Then slices were stored in liquid nitrogen and homogenized in cold 0.32 M sucrose containing 1 mM HEPES, 1 mM $MgCl_2$, 1 mM $NaHCO_3$, 20 mM sodium pyrophosphate, 20 mM β-phosphoglycerol, 0.2 mM dithiothreitol, 1 mM EDTA, 1 mM EGTA, 50 mM NaF, 1 mM Na_3VO_4, and 1 mM *p*-nitrophenyl phosphate, pH 7.4, in the presence of the following protease inhibitors and phosphatase inhibitors: 1 mM phenylmethylsulfonyl fluoride (PMSF), 5 μg/ml aprotinin, 5 μg/ml leupeptin, 5 μg/ml pepstatin A, and 16 μg/ml benzamidine. The homogenate was centrifuged at 1,000 × *g* for 10 min. Some of the resulting supernatant was left as the total protein fraction, and the remainder was centrifuged at 3,000 × *g* for 15 min. The supernatant was the cytoplasmic fraction. The pellet was resuspended in 8 ml of hypotonic buffer (in the presence of proteases inhibitors) and centrifuged at 100,000 × *g* for 1 h. The resultant pellet was resuspended in 8 ml of buffer containing 75 mM KCl and 1% Triton X-100 and centrifuged at 100,000 × *g* for 1 h. The final pellet was sonicated three times in 20 mM HEPES. This fraction was referred to as the "Triton X-100-insoluble fraction." The sample was stored at −80 °C. The Triton X-100-insoluble fraction was used instead of the classical PSD because the amount of hippocampal slices was very limited.

Immunoprecipitation—Different fractions (total protein fraction, cytoplasmic fraction, and Triton X-100-insoluble fraction) (200 μg of protein) were incubated overnight at 4 °C in immunoprecipitation buffer (0.05 M HEPES, pH 7.4 containing 10% glycerol, 0.15 M NaCl, 1% Triton X-100, 0.5% Nonidet P-40, and a 1 mM concentration each of EDTA, EGTA, PMSF, and Na_3VO_4) with antibody against CaMKII (2 μg) or CaM (2 μg), respectively. Then Protein A-agarose beads were added, gently vortexed, and incubated for 2 h at 4 °C. The beads were recovered by centrifugation at 10, 000 × *g* and gently washed three times with immunoprecipitation buffer. SDS sample loading buffer for SDS-PAGE was added, and the mixture was incubated at 100 °C for 5 min. Beads were centrifuged, and the supernatants were applied to 7.5% SDS-PAGE.

Immunoblotting—Equal amounts of protein (20 μg) or proteins purified by immunoprecipitation were separated by 7.5% SDS-PAGE and electrotransferred onto nitrocellulose membranes (0.45 mm; BioTrance NT, Ann Arbor, MI) for immunoblotting. Membranes were blocked with 3% (w/v) BSA (fraction V) in wash buffer (10 mM Tris, pH 7.4, 0.1% (w/v) Tween 20, and 100 mM NaCl) for 1 h at room temperature. Blotted proteins were probed with the following primary antibodies: goat anti-NR2A (1:750; Santa Cruz Biotechnology), mouse anti-NR2B (1:500; a gift from Professor Jianhong Luo of Zhejiang University, Hangzhou, China), rabbit anti-phosphorylated CaMKII (p-CaMKII) (Thr-286) (1:750; Cell Signaling Technology), rabbit anti-tubulin (1:800; bioWORLD), rabbit anti-phospho-neuromodulin (anti-p-neuromodulin; 1:1000, Millipore), rabbit anti-neuromodulin (1:800; Santa Cruz Biotechnology), and goat anti-CaM (1:800; Santa Cruz Biotechnology). Secondary antibodies were donkey anti-rabbit or sheep anti-mouse IgG and rabbit anti-goat IgG HRP-conjugated antibodies. Signals were generated by enhanced chemiluminescence reagent (bioWORLD) according to the manufacturer's protocol and visualized by exposure using a Bio-Rad system. Quantification was performed using ImageJ. Results are expressed as -fold *versus* control.

Triple Immunofluorescence Staining—Fluorescent triple immunostaining was applied to determine the colocalization of

NR2A or NR2B, CaMKII, and PSD-95 in rat hippocampal slices. Slices were prepared and incubated for 15 min with PMA (0.5 μM) following preincubation with Tat-NR2A (0.5 μM), Tat-NR2B (0.5 μM), or Myr-AIP (1 μM) for 20 min. Fifteen minutes after each treatment, slices were fixed in ice-cold 4% paraformaldehyde overnight, dehydrated in 30% sucrose for 24 h at 4 °C, and sectioned at 40 μm on a freezing microtome (Leica CM1900). Sections were permeabilized in 0.3% Triton X-100 for 60 min and then blocked with 10% cattle serum for 60 min. Sections were then incubated with goat anti-NR2A or -NR2B antibody (1:50; Santa Cruz Biotechnology), rabbit anti-CaMKII (1:100; Santa Cruz Biotechnology), and mouse anti-PSD-95 antibody (1:100; Santa Cruz Biotechnology) in PBS containing 10% cattle serum at 4 °C for 48 h. After they were thoroughly washed with PBS, sections were probed with FITC-, TRITC-, and Cy™5-conjugated secondary antibodies (1:500; Jackson ImmunoResearch Laboratories) at 37 °C for 2 h or 4 °C overnight. The sections were mounted with a mounting medium (Vectashield, Vector Laboratories) after rinsing with PBS.

Image Acquisition and Quantification—Confocal imaging was performed as described previously (26). The images were captured using confocal microscopy (Olympus FV1000) with a 60× oil immersion lens. A series of optical sections were collected at steps of 0.50 μm and a resolution of 1024 × 1024 pixels. Each image was collected by averaging four scans. Because of the variability in brightness, it was necessary to use different gain and contrast settings for different cells. To control for this, all measurements were expressed in terms of ratios. All measurements were performed using NIH ImageJ software. The fluorescence intensity ratio of NR2A/NR2B and CaMKII to PSD-95 was expressed in arbitrary units of fluorescence per unit area as described previously (27). To quantify the staining, sections from three animals were used for quantitative analysis. Generally, three to four images of each slice were averaged to determine a value for the slice. A close-up view was obtained from one segment of an apical dendrite (about 50–150 μm away from the cell body layer; see Ref. 28). The data were analyzed with ANOVA least significant difference (LSD) for statistical significance and are expressed as means ± S.E.

Drugs—1,2,3,4-Tetrahydro-6-nitro-2,3-dioxobenzo[*f*]-quinoxaline-7-sulfonamide, phorbol 12-myristate 13-acetate, and chelerythrine chloride were from Sigma-Aldrich. Bicuculline methiodide was from Tocris. Myristoylated-AIP was from Biomol. Tat-NR2A and Tat-NR2B were from AC Scientific Inc.

Data Analysis—All population data are expressed as mean ± S.E. Within-group comparisons were performed using paired-sample *t* tests, and differences between groups were compared using independent-sample *t* tests and ANOVA LSD comparisons. A one-way ANOVA test was used when equal variances were assumed. Differences were considered significant when p was <0.05, and the significance for homogeneity of variance test was set at 0.1.

RESULTS

PKC Activation Elevated Level of Autophosphorylated CaMKII and Its Association with NMDARs—Previous studies demonstrated that PKC activation promotes NMDAR trafficking to the cell surface (3, 4). It is still uncertain whether PKC activation enhances NMDAR targeting to postsynaptic sites, especially for the NR2 subunits of which the composition is suggested to control synaptic plasticity by regulating binding to CaMKII (25). We first examined the effect of the PKC agonist PMA (0.5 μM) on postsynaptic trafficking of both NR2A and NR2B subunits and CaMKII autophosphorylation in hippocampal slices. Using a Western blot assay of the Triton X-100-insoluble fraction of hippocampal tissue (12), which roughly represents the subcellular fraction at postsynaptic sites (12, 29), we found a dramatic elevation of postsynaptic expression of NR2A, NR2B, autophosphorylated CaMKII, and CaMKII upon PKC activation by 15-min PMA treatment (NR2A, 1.79 ± 0.17, $n = 5$, $p < 0.01$; NR2B, 1.60 ± 0.07, $n = 5$, $p < 0.01$; p-CaMKII, 1.82 ± 0.16, $n = 5$, $p < 0.01$; CaMKII, 1.76 ± 0.11, $n = 5$, $p < 0.01$; ANOVA LSD test; Fig. 1, *A* and *B*). Interestingly, this effect was totally abolished by the selective CaMKII antagonist Myr-AIP (1 μM; compared with control, $p > 0.05$). By contrast, Myr-AIP alone failed to exert any obvious effect. The concurrent increases of postsynaptic expression of NR2 subunits and CaMKII point to a closed association

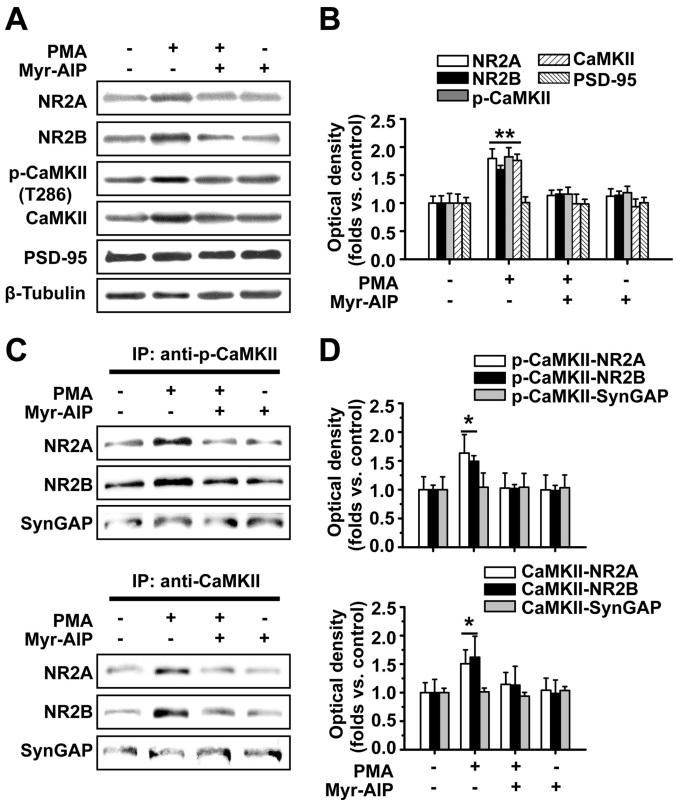

FIGURE 1. **PKC activator PMA potentiates CaMKII autophosphorylation, NR2 subunit expression, and association between CaMKII and NR2 subunits at postsynaptic sites: Western blot and co-IP evidence.** *A*, PMA treatment promotes postsynaptic expression of NR2A and NR2B subunits and CaMKII and CaMKII autophosphorylation as represented by Western blot assay. This potentiating effect was completely blocked by the CaMKII antagonist Myr-AIP (1 μM). By contrast, Myr-AIP alone failed to exert any obvious effect. *B*, statistical plot of data displaying the effects of PMA and Myr-AIP on postsynaptic NR2 expression and autophosphorylation of CaMKII. *C*, co-IP assay reveals the potentiating effect of the association between NR2A or NR2B and CaMKII or p-CaMKII in postsynaptic sites that was totally abolished by Myr-AIP. *D*, statistical plot of data displaying the effects of PMA and Myr-AIP as shown in *C*. *, $p < 0.05$; **, $p < 0.01$ compared with control; ANOVA LSD test. *Bars* represent mean ± S.E. *Error bars* represent S.E. and are derived from independent sets of experiments.

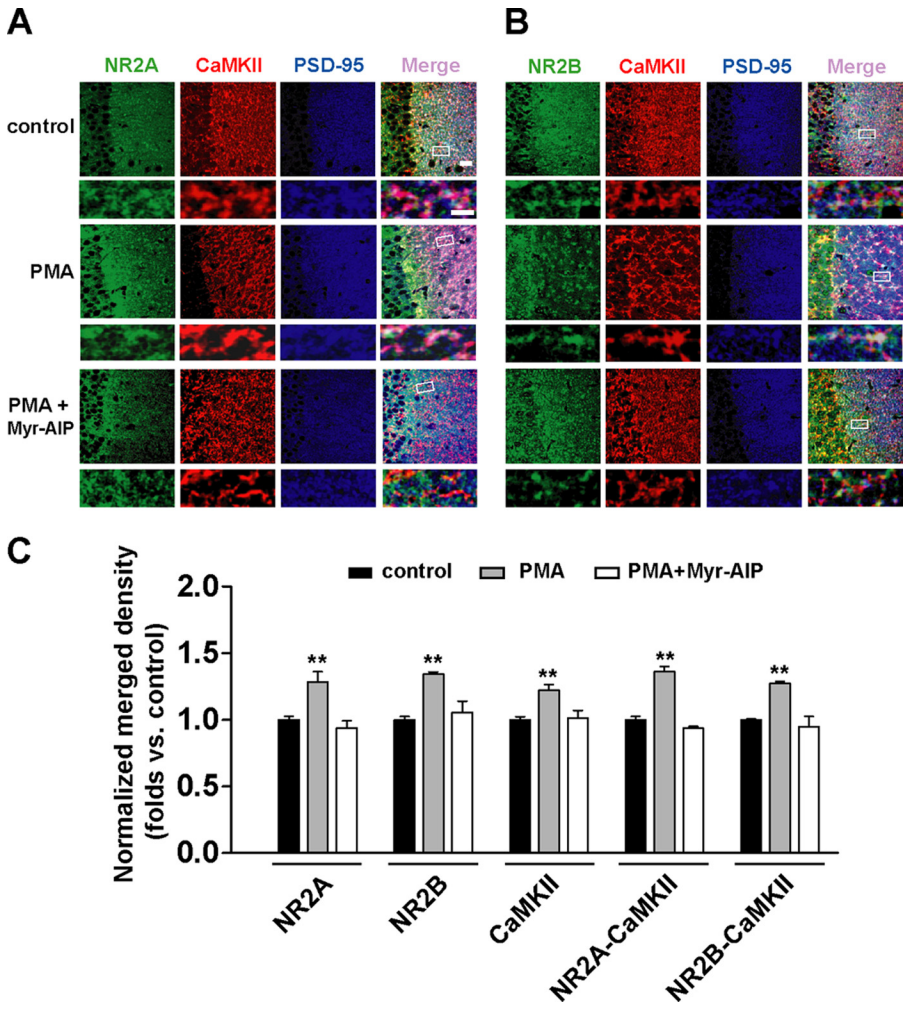

FIGURE 2. **PKC activator PMA potentiates postsynaptic NR2 subunit expression and association with CaMKII: immunofluorescence evidence.** *A*, triple immunofluorescence labeling of NR2A (*left*) and CaMKII (*middle left*) with PSD-95 (*middle right*) in hippocampal CA1 neurons in slices. *Right*, overlay. $n = 9$. *Bar*, 20 μm. Higher magnification of dendritic branches is shown in the *lower panels*. *Bar*, 2 μm. The *boxes* in the *merge column* indicate corresponding magnified regions. PMA treatment promotes postsynaptic colocalization between NR2A subunit and CaMKII. This potentiating effect was totally abolished by the CaMKII antagonist Myr-AIP (1 μM). *B*, similar experiments as shown in *A* except NR2B was substituted for NR2A. $n = 10$. *C*, statistical plots of data displaying the effects of PMA and Myr-AIP as shown in *A* and *B*, respectively. **, $p < 0.01$ compared with control; one-way ANOVA LSD test. *Error bars* represent S.E.

between these molecules at postsynaptic sites. Indeed, an enhanced association between NR2A or NR2B and CaMKII or p-CaMKII was detected using a co-immunoprecipitation (co-IP) assay (NR2A/CaMKII, 1.51 ± 0.24, $n = 6$, $p < 0.05$; NR2B/CaMKII, 1.62 ± 0.36, $n = 6$, $p < 0.05$; NR2A/p-CaMKII, 1.63 ± 0.32, $n = 6$, $p < 0.05$; NR2B/p-CaMKII, 1.49 ± 0.10, $n = 6$, $p < 0.05$; ANOVA LSD test; Fig. 1, *C* and *D*) that was blocked by preincubating the slices with the CaMKII antagonist Myr-AIP (1 μM) for 20 min (compared with control, $p > 0.05$). The absence of change in the association of another postsynaptic protein, SynGAP, to CaMKII upon PKC activation ensures the specificity for NR2-CaMKII complex. A control with an irrelevant IgG was also obtained to assess the specificity of the IP (supplemental Fig. 1). Moreover, we stimulated PKC by physiological stimuli to determine whether neurotransmitter effects on NMDAR insertion also require CaMKII (supplemental Fig. 2). We first used a physiological stimulation protocol (θ-burst stimulation; five trains of burst with four pulses at 100 Hz at 200-ms intervals repeated four times at intervals of 10 s; see Ref. 30) previously proved to be effective in induction of LTP of NMDAR-mediated EPSCs (LTP_{NMDA}) to ensure the enhancement of functional NMDA receptors. This enhancement of NMDAR-mediated EPSCs could be largely attenuated by exocytosis blocker tetanus toxin (TeTx; 0.1 μM), suggesting that insertion of new NMDARs accounts for this enhancement. Then we demonstrated that this physiological stimulation protocol indeed activated PKC. Finally, we found that the CaMKII antagonist Myr-AIP could block NMDAR functional enhancement induced by physiological stimuli. These results confirm that neurotransmitter effects on NMDAR insertion also require CaMKII.

We further used an immunofluorescence assay to doubly confirm the above finding by PKC activation. Using PSD-95 as a postsynaptic marker, we detected a similar elevation in postsynaptic expression of NR2A, NR2B, and CaMKII (NR2A, 1.28 ± 0.03, $n = 9$, $p < 0.01$; NR2B, 1.34 ± 0.02, $n = 10$, $p < 0.01$; CaMKII, 1.22 ± 0.04, $n = 15$, $p < 0.01$; Fig. 2, *A*–*C*) as well as elevation in association between NR2 subunits and CaMKII in postsynaptic sites represented by increased colocalization between them (NR2A/CaMKII, 1.23 ± 0.03, $n = 9$, $p < 0.01$;

NR2B/CaMKII, 1.25 ± 0.02, $n = 10$, $p < 0.01$; ANOVA LSD test; Fig. 2, *A–C*). These potentiating effects were also antagonized by preincubating the slices with the CaMKII antagonist Myr-AIP (1 μM) for 20 min (compared with control, $p > 0.05$). Taken together, these results suggest that PKC elicits concurrent potentiation in both CaMKII autophosphorylation and association between CaMKII and NMDARs at postsynaptic sites, supporting the interpretation that PKC may exert this potentiating effect through triggering CaMKII autophosphorylation and the subsequent greatly increased binding to NR2 subunits.

Possible Mechanisms for PKC Activation—We further determined how PKC activation elicits CaMKII autophosphorylation and its association with NMDARs. We found that either low extracellular Ca^{2+} concentration (0.01 mM) or the selective NMDA receptor antagonist AP5 (50 μM) could totally abolish PKC-induced potentiation of CaMKII autophosphorylation and NMDAR subunit expression at postsynaptic sites (low Ca^{2+}: NR2A, 0.98 ± 0.13, $n = 5$, $p > 0.05$; NR2B, 1.08 ± 0.12, $n = 5$, $p > 0.05$; p-CaMKII, 0.97 ± 0.14, $n = 5$, $p > 0.05$; CaMKII, 0.95 ± 0.15, $n = 5$, $p > 0.05$; ANOVA LSD test; AP5: NR2A, 0.97 ± 0.12, $n = 5$, $p > 0.05$; NR2B, 0.96 ± 0.10, $n = 5$, $p > 0.05$; p-CaMKII, 0.96 ± 0.12, $n = 5$, $p > 0.05$; CaMKII, 0.96 ± 0.15, $n = 5$, $p > 0.05$; ANOVA LSD test; Fig. 3, *A* and *B*). These data suggest that Ca^{2+} influx through NMDAR upon PKC activation is necessary for PMA-induced CaMKII autophosphorylation. Because PKC phosphorylates CaM-binding proteins that in some cases lead to release of bound CaM (31), which could then increase activation of CaMKII even without modifying basal Ca^{2+} stimuli, we also examined whether PKC phosphorylates CaM-binding proteins that lead to release of bound CaM. We found that PKC activation indeed phosphorylated the CaM-binding protein neuromodulin and decreased its association with CaM accompanied by a concurrent increase in association between CaM and CaMKII at postsynaptic sites (phosphoneuromodulin: 1.68 ± 0.26, $n = 5$, $p < 0.05$; CaM-neuromodulin: 0.72 ± 0.08, $n = 6$, $p < 0.05$; CaM-CaMKII: 1.69 ± 0.16, $n = 6$, $p < 0.05$; Fig. 3, *E* and *F*). These results suggest that the PKC-induced dissociation between CaM and neuromodulin and increase of cytosolic CaM might contribute to the CaMKII autophosphorylation.

PKC Promotes Functional NMDAR Insertion into Postsynaptic Membrane—To further investigate the functional implications of the above potentiating effects of PKC activation, we used whole-cell patch clamp recording in hippocampal CA1 neurons to detect possible changes in NMDAR-mediated EPSCs (NMDA EPSCs) accompanying the above enhancement of postsynaptic NMDAR expression and association between NR2 subunits and CaMKII. Evoked NMDA currents were recorded when the cells were held at +40 mV with the specific AMPA receptor antagonist 1,2,3,4-tetrahydro-6-nitro-2,3-dioxobenzo[*f*]quinoxaline-7-sulfonamide (10 μM) in the perfusion medium. PKC activation by intracellular loading of recorded cells with PMA (0.2 μM) significantly increased the amplitude of NMDA EPSCs at 30 min after PMA treatment (1.68 ± 0.19, $n = 8$, $p < 0.01$, paired-sample *t* test; Fig. 4*A*), supporting a functional role of newly inserted NMDARs in the postsynaptic sites. Because both NR2A and NR2B have very

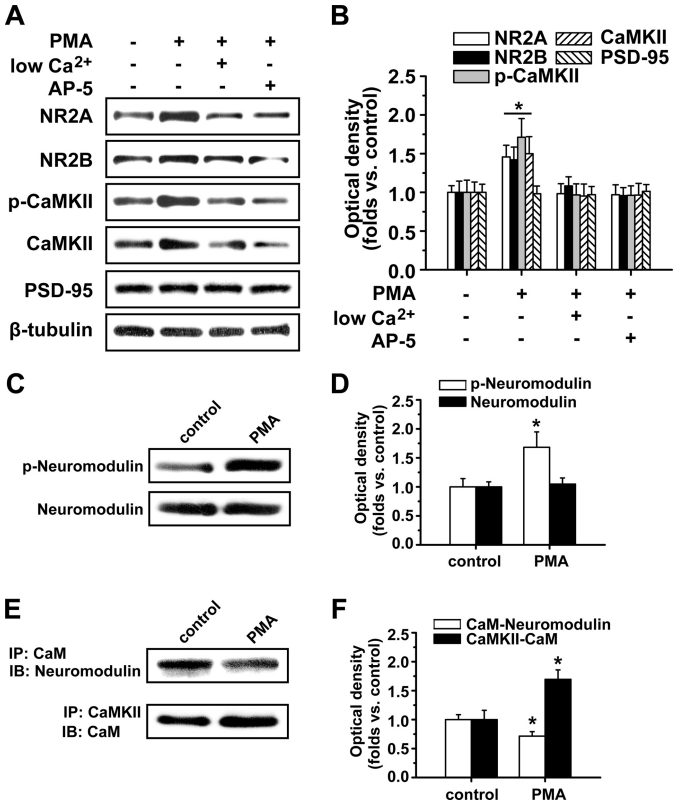

FIGURE 3. **Possible mechanisms for PKC activation**. *A*, low extracellular Ca^{2+} concentration (0.01 mM) or selective NMDA receptor antagonist AP5 (50 μM) totally abolished PKC-induced potentiation of CaMKII autophosphorylation and NMDAR subunit expression at postsynaptic sites. *B*, statistical plots of data displaying the effects of low extracellular Ca^{2+} concentration and AP5 as shown in *A*. *C*, PKC activation by PMA treatment activated and elicited phosphorylation of the CaM-binding protein neuromodulin. *D*, statistical plots of data displaying similar results as shown in *C*. *E*, PKC activation by PMA treatment induced decreased association between CaM and neuromodulin accompanied by a concurrent increase in association between CaM and CaMKII at postsynaptic sites. *F*, statistical plots of data from experiments such as those shown in *E*. *, $p < 0.05$ compared with control; one-way ANOVA LSD test. *p-neuromodulin*, phospho-neuromodulin; *IB*, immunoblot.

long cytoplasmic tails that have been shown to play critical roles in directing the trafficking to and stabilization of synaptic sites (32), they are good candidates to participate in controlling the number and composition of NMDARs at a synapse. The different NR2 subunits (NR2A–NR2D) display distinct kinetic and pharmacological properties in heteromeric receptors. The NR1/NR2A composition displays a faster decay constant than NR1/NR2B receptors (33). We then investigated whether PKC activation by PMA induces a change in the decay time of NMDA EPSCs, which may be an indicator of change in NR2 subunit composition. Interestingly, we found that a prolonged decay of NMDA EPSCs at 30 min after PMA treatment (1.43 ± 0.11, $n = 8$, $p < 0.01$, paired-sample *t* test; Fig. 4*A*) accompanied the increase in amplitude, pointing to an increase of at least the functional NR2B component of NMDARs.

To further determine whether the prolongation of EPSCs decay is due to an increase of the NR2B component alone or concurrent changes in both NR2A and NR2B components, we perfused the slice with the NR2B antagonist ifenprodil (3 μM) to check whether the ifenprodil-insensitive NR2A component changed. As shown in Fig. 4*B*, we detected a significant increase

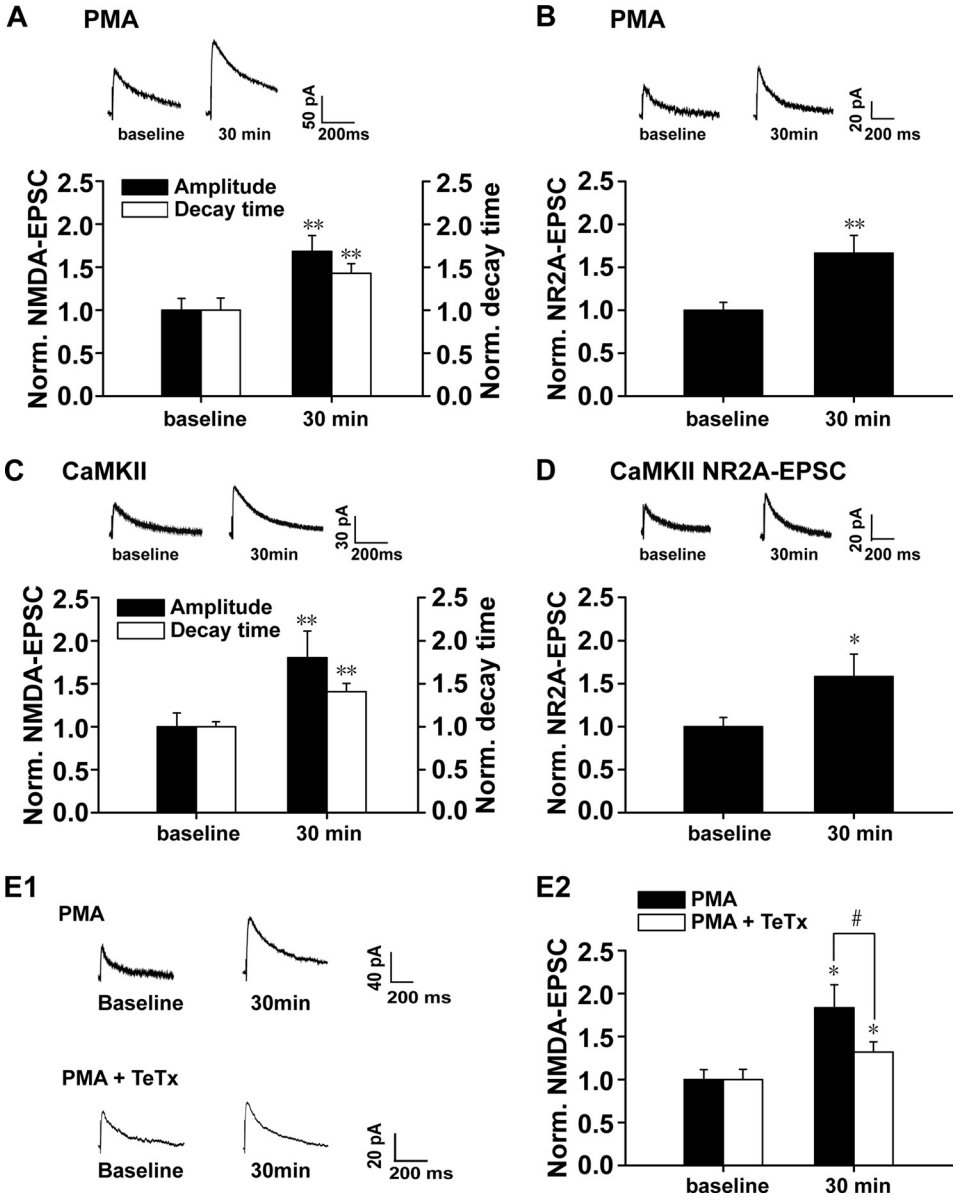

FIGURE 4. **PKC activation promotes postsynaptic trafficking and insertion of functional NMDARs.** *A*, statistical plots of data reveal that PKC promotes both amplitude and decay time of NMDAR-mediated synaptic responses. *B*, PKC promotes synaptic responses mediated by NMDAR NR2A subunit. Synaptic responses mediated by NMDAR NR2A component were isolated by a selective antagonist of NR2B subunit, ifenprodil (3 μM). *C*, CaMKII activation promotes both amplitude and decay time of NMDAR-mediated synaptic responses. CaMKII activation was achieved by loading recorded cells with the active form of CaMKII (0.2 μM). *D*, CaMKII activation promotes synaptic responses mediated by NMDAR NR2A subunit. *, $p < 0.05$; **, $p < 0.01$ compared with base line; one-way ANOVA LSD test. *E1*, sample traces of evoked NMDAR-mediated synaptic responses when cells were held at +40 mV. *Top panel*, PKC activation by PMA-induced potentiation of NMDAR-mediated currents. *Bottom panel*, potentiation of NMDA currents was partially antagonized by SNARE-dependent exocytosis blocker TeTx (0.1 μM). *E2*, statistical plots of data displaying the effect of PMA and TeTx as shown in *E1*. These data suggest that postsynaptic insertion of functional NMDARs at least partially contributes to the potentiation of NMDA currents induced by PKC activation. *, $p < 0.05$ compared with base line; #, $p < 0.05$ compared with PMA treatment group; one-way ANOVA LSD test. *Norm.*, normalized.

in the functional NR2A component of NMDARs after PMA treatment (1.67 ± 0.21, $n = 11$, $p = 0.001$, paired-sample *t* test; Fig. 4*B*). Therefore, PKC-induced potentiation of NMDAR EPSCs is due to a concurrent increase of functional NR2A and NR2B components. Because the NR1/NR2A composition displays a faster decay constant than NR1/NR2B receptors (33), the present finding of prolonged decay support the interpretation of a relatively greater contribution of the NR2B subunit than that of the NR2A subunit to the increased amplitude. Similar potentiation in amplitude and decay time of NMDA EPSCs was observed upon CaMKII activation by intracellularly loading recorded CA1 neurons with the activated form of CaMKII (0.2 μM; kindly provided by Dr. Thomas R. Soderling; NR2B: amplitude change, 1.80 ± 0.31; $n = 8$, $p < 0.01$; decay time change, 1.41 ± 0.10; $n = 8$, $p < 0.01$; NR2A: amplitude change, 1.58 ± 0.26; $n = 11$, paired-sample *t* test; Fig. 4, *C* and *D*).

PKC-induced potentiation of NR2A- or NR2B-mediated NMDA currents could be caused by both pre- and postsynaptic factors. It was still uncertain whether NMDAR trafficking contributed, at least in part, to the above enhancement of functional NMDA currents. To test this possibility, we loaded recorded cells with PMA and SNARE-dependent exocytosis

blocker TeTx (0.1 μM) to block NMDAR trafficking (20, 34, 35). We found that this treatment partially (although not totally) antagonized the potentiation of NMDA currents induced by PKC activation (PMA + TeTx, 1.32 ± 0.12, $n = 5$, $p < 0.05$ compared with PMA and $p < 0.01$ compared with base line, paired-sample t test; Fig. 4, *E1* and *E2*). Combined with the Western blot, co-IP, and immunofluorescence data, these findings strongly suggest that PKC promotes functional NMDAR insertion into postsynaptic membrane.

Interfering with NR2-CaMKII Association Blocks Postsynaptic Expression and Functional Insertion of NMDARs—To determine whether increased association between NMDAR NR2 subunits and CaMKII upon PKC activation is required for PKC-induced NMDAR trafficking, we disturbed NR2-CaMKII association with constructed short peptides that were targeted directly to the binding sites between them and assessed how these treatments affected the postsynaptic expression and functional insertion of NMDARs. It is reported that NR2A directly binds with αCaMKII at specific domain amino acids 1413–1419 within its C terminus, whereas NR2B associates with αCaMKII at specific domain amino acids 1290–1309 (12, 36, 37). Site-directed mutagenesis of NR2A residues 1413–1419 of the cytosolic tail inhibits αCaMKII binding and promotes dissociation of the αCaMKII-NR2A complex (12), and site-directed mutagenesis of the region containing NR2B residues 1290–1309 promotes dissociation of the αCaMKII-NR2B complex (38). The peptides we constructed here had exactly the same sequence of amino acids at the NR2 binding sites and thus could competitively antagonize binding between NR2A or NR2B and CaMKII (12, 38). Tat protein (Tyr-Gly-Arg-Lys-Lys-Arg-Arg-Gln-Arg-Arg-Arg), which was obtained originally from the cell membrane transduction domain of the human immunodeficiency virus type 1 (HIV-1), was fused to the constructed peptides and resulted in fusion peptides Tat-NR2A and Tat-NR2B. This manipulation allowed the constructed peptides to easily cross the membrane and exert their effects intracellularly (39). Tat-NR2A (0.5 μM) not only completely blocked PKC-induced potentiation of NR2A expression and NR2A-CaMKII association (NR2A, 1.10 ± 0.12, $n = 5$, $p > 0.05$ compared with control; NR2A-CaMKII, 1.11 ± 0.10, $n = 5$, $p > 0.05$, compared with control, one-way ANOVA LSD test) but also partially blocked enhancement in NR2B or p-CaMKII expression and NR2B-CaMKII association at postsynaptic sites (NR2B, 1.17 ± 0.08, $n = 5$, $p < 0.05$, compared with control; p-CaMKII, 1.19 ± 0.12, $n = 5$, $p < 0.05$; NR2B-CaMKII, 1.24 ± 0.09, $n = 5$, $p < 0.05$, one-way ANOVA LSD test) as indicated by both Western blot and co-IP assay (Fig. 5, *A–D*). Furthermore, Tat-NR2B (0.5 μM) treatment completely blocked translocation of both NR2 subunits and CaMKII (NR2A, 1.10 ± 0.12, $n = 5$; NR2B, 0.92 ± 0.07, $n = 5$; p-CaMKII, 0.93 ± 0.24, $n = 5$, $p > 0.05$ compared with control, one-way ANOVA LSD test) and blocked the increase in association between them induced by PKC activation (NR2A-CaMKII, 1.08 ± 0.12, $n = 5$; NR2B-CaMKII, 0.99 ± 0.12, $n = 5$, $p > 0.05$ compared with control, one-way ANOVA LSD test; Fig. 5, *A–D*). By contrast, without PKC activation, both Tat-NR2 peptides used to interfere with the association between CaMKII and NMDAR failed to display obvious effects on CaMKII autophosphorylation and NR2 subunit expression at postsynaptic sites (Fig. 5, *A* and *B*).

One interesting finding emerged when we examined the quantity of NR2 subunits and CaMKII remaining in the cytoplasm after interference experiments. In contrast to the blockade by Tat-NR2A or Tat-NR2B on the PKC-induced enhancement of postsynaptic NMDAR expression, the quantity of both NR2A and NR2B in the cytoplasm as assayed by Western blot displayed a marked increase (NR2A/Tat-NR2A, 1.53 ± 0.13, $n = 5$, $p < 0.05$; NR2B/Tat-NR2A, 1.26 ± 0.11, $n = 5$, $p < 0.05$ compared with the PMA-treated group; NR2A/Tat-NR2B, 1.47 ± 0.14, $n = 5$, $p < 0.05$; NR2B/Tat-NR2B, 1.23 ± 0.12, $n = 5$, $p < 0.05$, one-way ANOVA LSD test; Fig. 5, *A* and *B*). PMA alone failed to exert any influence on the cytoplasmic NR2 subunits ($p > 0.05$). In addition, the cytoplasmic p-CaMKII did not change upon Tat-NR2A or Tat-NR2B blockade. The absence of change in p-CaMKII could be due to its instability after blocking the NR2-CaMKII association. These data suggest that the binding between NR2 subunits and CaMKII is a critical prerequisite for their postsynaptic translocation. NR2 subunits and CaMKII might co-translocate to postsynaptic sites in the form of CaMKII-NMDAR complexes (also see "Discussion").

We then used a triple immunofluorescence staining assay in slices to doubly assess the results of interfering with the association between NR2 subunits and CaMKII. Consistent with the above findings using Western blot and co-IP, we found that Tat-NR2A completely blocked the increase of postsynaptic NR2A and CaMKII (NR2A, 1.00 ± 0.05, $n = 12$, $p > 0.05$; CaMKII, 1.00 ± 0.04, $n = 15$, $p > 0.05$) as well as enhanced colocalization between NR2A and CaMKII at postsynaptic sites upon PKC activation by PMA (0.92 ± 0.03, $n = 12$, $p > 0.05$ compared with control, one-way ANOVA LSD test; Fig. 6, *A* and *C*) but partially blocked NR2B and the colocalization of NR2B and CaMKII (NR2B, 1.16 ± 0.03, $n = 10$, $p < 0.05$; NR2B/CaMKII, 1.14 ± 0.03, $n = 10$, $p < 0.05$ compared with control). Moreover, Tat-NR2B treatment completely blocked colocalization between both NR2 subunits and CaMKII induced by PKC activation ($p > 0.05$ compared with control; Fig. 6, *B* and *C*). Taken together, these results clearly demonstrate that a stable association between both NR2 subunits and CaMKII is required for their postsynaptic trafficking.

We further examined the functional implications of interfering with NR2-CaMKII association on NMDAR surface expression by monitoring synaptic NMDA EPSCs. Preincubating slices with Tat-NR2A (0.5 μM) for 30 min partially antagonized the PKC-induced potentiation of amplitude and decay time of NMDA EPSCs (amplitude, 1.55 ± 0.02; decay, 1.66 ± 0.04; $n = 7$; $p < 0.05$ compared with PMA-treated group, one-way ANOVA LSD test; Fig. 7, *A* and *B*), whereas treating slices with Tat-NR2B (0.5 μM) completely abolished PKC-induced potentiation (amplitude, 1.12 ± 0.18; decay, 1.03 ± 0.07; $n = 7$, $p > 0.05$ compared with base line, one-way ANOVA LSD test; Fig. 7, *A* and *B*). Similar results with Tat-NR2A or Tat-NR2B were obtained in cells treated with the activated form of CaMKII (0.2 μM; Tat-NR2A: amplitude, 1.54 ± 0.25; decay, 1.60 ± 0.07; $n = 8$, $p < 0.05$ compared with group treated with activated CaMKII; Tat-NR2B, amplitude, 1.04 ± 0.11; decay, 1.07 ± 0.13; $n = 8$, $p > 0.05$ compared with base line, one-way ANOVA LSD

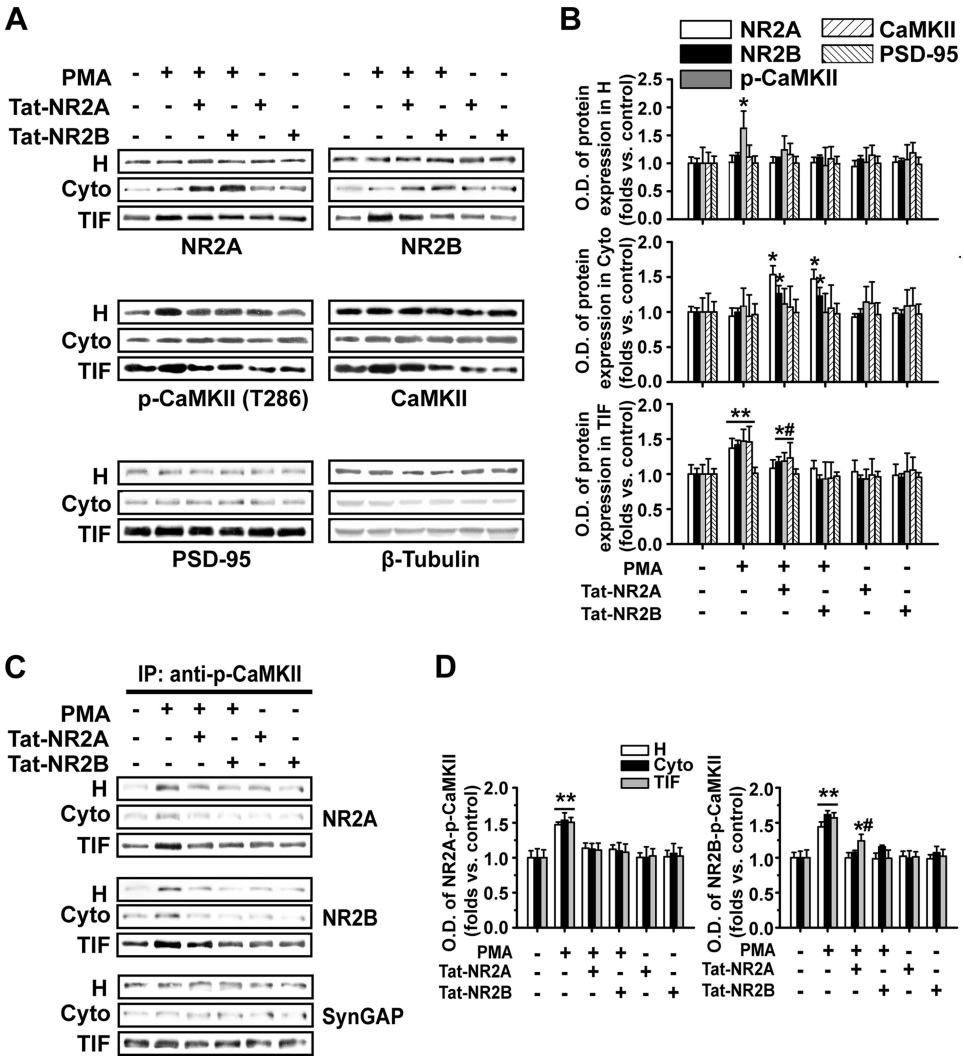

FIGURE 5. **Disturbing the association between NR2 subunits and CaMKII blocks enhanced postsynaptic NMDAR trafficking upon PKC activation: Western blot and co-IP evidence.** *A*, disturbing the association between NR2 subunits and CaMKII with membrane-permeable peptide Tat-NR2A or Tat-NR2B antagonized the potentiation of postsynaptic expression of NR2 subunits and CaMKII autophosphorylation induced by PMA as represented by Western blot assay. By contrast, either of the Tat-NR2 peptides alone failed to exert any obvious effect. *H*, total protein fractions; *Cyto*, cytoplasmic fractions; *TIF*, Triton X-100-insoluble fractions. *B*, statistical plots of data from experiments such as those shown in *A*. *C*, co-IP assay revealed the antagonizing effects of Tat-NR2A or Tat-NR2B on potentiation of association between NR2A or NR2B and CaMKII induced by PMA at postsynaptic sites. *D*, statistical plots of data from experiments such as those shown in *C*. *, $p < 0.05$; **, $p < 0.01$ compared with control; #, $p < 0.05$ compared with PMA-treated group; one-way ANOVA LSD test.

test; Fig. 7, *C* and *D*). By contrast, without PKC activation, both Tat-NR2 peptides failed to display obvious effects on NMDA EPSCs (supplemental Fig. 3). These results were fully consistent with the Western blot and immunofluorescence data showing more influence on NR2A than on NR2B by Tat-NR2A or CaMKII activation. Because both Tat-NR2A and Tat-NR2B failed to have any effect on presynaptic transmitter release (data not shown), these data strongly suggest that NR2-CaMKII association is essential for postsynaptic addition of functional NMDARs.

Interfering with NR2-CaMKII Association Blocks PKC-induced Synaptic Plasticity—Many forms of synaptic plasticity depend on NMDA receptor activation and the subsequent increase of intracellular Ca^{2+} (40–42). Thus, alteration in NMDAR function caused by interfering with NR2-CaMKII association might lead to changes in synaptic plasticity mediated by AMPA receptors. To further elucidate the functional consequences of interfering with NR2 subunits and CaMKII association in AMPAR-mediated synaptic plasticity, we determined how Tat-NR2A and Tat-NR2B affected synaptic plasticity induced by PKC or CaMKII activation. PKC or CaMKII activation was achieved by intracellularly loading recorded neurons with PMA (0.2 μM) or the active form of CaMKII (0.2 μM), respectively, each of which consistently produced LTP of AMPAR-mediated synaptic responses (PMA-treated group, 1.62 ± 0.06, $n = 6$; CaMKII-treated group, 1.81 ± 0.08, $n = 5$; $p < 0.001$ compared with base line, one-way ANOVA LSD test; Fig. 8*A*). In addition, both Tat-NR2A and Tat-NR2B completely abolished LTP induced by PKC activation (Tat-NR2A, 0.97 ± 0.03, $n = 6$; Tat-NR2B, 1.00 ± 0.04, $n = 6$; $p > 0.05$ compared with base line; Fig. 8, *A* and *B*). Similar effects with Tat-NR2A and Tat-NR2B were also found on LTP produced by CaMKII activation via intracellular loading of the active form of CaMKII (Tat-NR2A, 0.97 ± 0.04, $n = 6$; Tat-NR2B, 0.99 ± 0.04, $n = 6$; $p > 0.05$ compared with base line; Fig. 8, *C* and *D*). By contrast, preincubation of slices with Tat-NR2A or Tat-NR2B

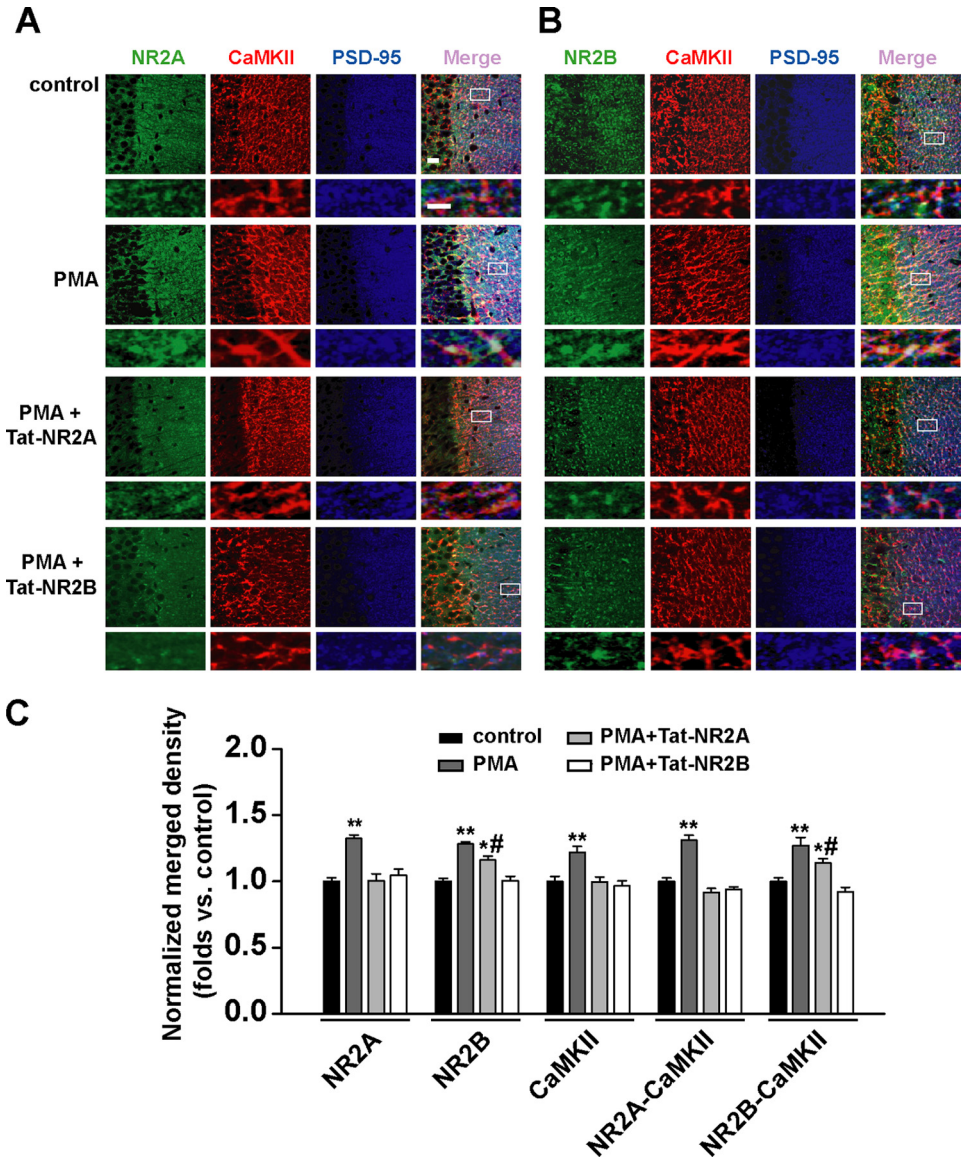

FIGURE 6. **Disturbing the association between NR2 subunits and CaMKII blocks enhanced postsynaptic NMDAR trafficking upon PKC activation: immunofluorescence evidence.** *A*, triple immunofluorescence labeling of NR2A (*left*) and CaMKII (*middle left*) with PSD-95 (*middle right*) in hippocampal CA1 neurons in slices. *Right*, overlay. $n = 12$. *Bar*, 20 μm. Higher magnification of dendritic branches is shown in the *lower panels*. *Bar*, 2 μm. The *boxes* in the *merge column* indicate corresponding magnified regions. Disturbing the association between NR2 subunits and CaMKII with membrane-permeable peptide Tat-NR2A or Tat-NR2B antagonized the potentiation of postsynaptic colocalization of NR2A subunits and CaMKII induced by PMA. *B*, similar experiments as in *A* except NR2B was substituted for NR2A. $n = 10$. *C*, statistical plots of data displaying the effect of Tat-NR2A and Tat-NR2B as shown in *A* and *B*, respectively. *, $p < 0.05$; **, $p < 0.01$ compared with control; #, $p < 0.05$ compared with PMA-treated group; one-way ANOVA LSD test.

alone did not affect basal AMPA receptor-mediated EPSCs (supplemental Fig. 3). These results suggest that the association between the NR2 subunit and CaMKII is critical for PKC- or CaMKII-induced LTP. Because disturbing the NR2-CaMKII association also blocked trafficking of both CaMKII and NMDARs into the postsynaptic membrane, these data reveal the possible correlation between postsynaptic NMDAR trafficking and AMPAR-mediated LTP production. Similar data on PKC- and CaMKII-induced LTP lend new support to the hypothesis that PKC and CaMKII act in series and at least partially share a common pathway in LTP induction. Moreover, we found that Tat-NR2 peptides could also block the induction of LTP mediated by the paired stimulation (supplemental Fig. 4).

Src Signaling Pathway Is Not Required for PKC-induced NMDAR Trafficking—The non-receptor tyrosine kinase Src participates in the induction of LTP at CA1 hippocampal synapses partly due to enhancing NMDA receptor activity (8, 43). In addition, PKC-dependent activation of the tyrosine kinase Src has been reported to be responsible for regulating the activity of NMDA channels (8). To determine whether Src also plays a role in PKC-induced potentiation of NMDA currents, which is at least in part caused by NMDAR trafficking and subsequent postsynaptic functional NMDAR insertion, we used the Src antagonist PP2 to assess how blocking Src function affects trafficking of NMDARs. We found that the trafficking of neither NMDARs nor CaMKII was influenced by PP2 (1 μM) or its

inactive analog, PP3 (1 μM), as indicated by the absence of changes in PKC-induced enhancement of postsynaptic expression of NR2 and CaMKII (PP2/NR2A, 1.62 ± 0.15; PP2/NR2B, 1.59 ± 0.22; PP2/p-CaMKII, 1.44 ± 0.41; $n = 4$; PP3/NR2A, 1.64 ± 0.25; PP3/NR2B, 1.69 ± 0.43; PP3/p-CaMKII, 1.46 ± 0.38; $n = 4$; $p > 0.05$ compared with PMA-treated group, one-way ANOVA LSD test; Fig. 9, *A* and *B*). Moreover, the increased association between NR2 and CaMKII induced by PKC was also unaffected by PP2 or PP3 application ($p > 0.05$; Fig. 9, *C* and *D*). Inconsistent with these biochemical data, however, PP2 partially suppressed the enhancement of amplitude but not decay time of NMDA currents (amplitude, 1.47 ± 0.07; $n = 6$, $p < 0.05$; decay time, 1.48 ± 0.17; $n = 6$, $p > 0.05$ compared with PMA-treated group; Fig. 9, *E* and *F*). The absence of change in decay time of NMDA current upon PP2 treatment could represent a proportional decrease in NR2A and NR2B components. These results suggest that the Src signaling pathway is not required for PKC-induced NMDAR trafficking. Src may regulate NMDA function through other mechanisms; for instance, Src might directly phosphorylate the NMDA channel and potentiate its gating as demonstrated by a previous study (8, 9, 43).

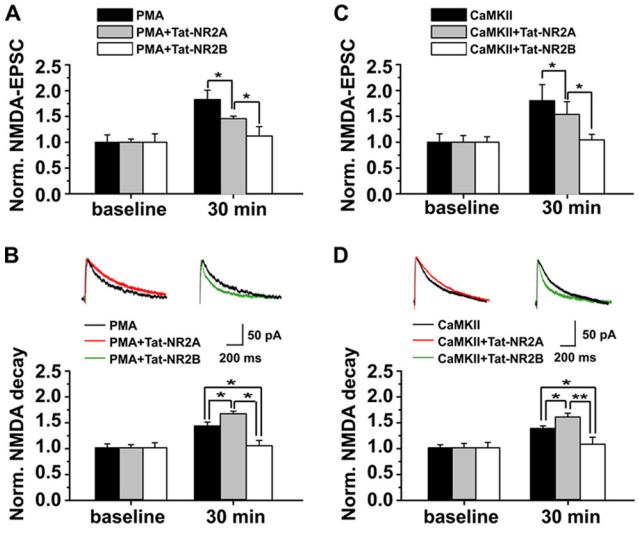

FIGURE 7. **Disturbing the association between CaMKII and NR2 subunits antagonizes postsynaptic trafficking and insertion of functional NMDARs induced by PKC or CaMKII activation.** *A*, disturbing the CaMKII-NR2 association suppressed the amplitude of NMDAR-mediated synaptic responses. NMDA currents were recorded at +40-mV voltage. Normalized NMDA currents were compared at base line and 30 min after PMA treatment. Tat-NR2A partially whereas Tat-NR2B completely blocked PKC-induced potentiation of NMDA currents. *B*, disturbing the CaMKII-NR2 association with Tat-NR2A or NR2B differentially modulated the decay time of NMDA currents. Tat-NR2A enhanced the decay time, whereas Tat-NR2B prolonged the decay time. *C* and *D*, similar data on amplitude (*C*) and decay time (*D*) of NMDA currents were obtained after CaMKII activation. *, $p < 0.05$; **, $p < 0.01$ compared with group treated with both PMA and Tat-NR2A (*PMA+Tat-NR2A*); one-way ANOVA LSD test. *Norm.*, normalized.

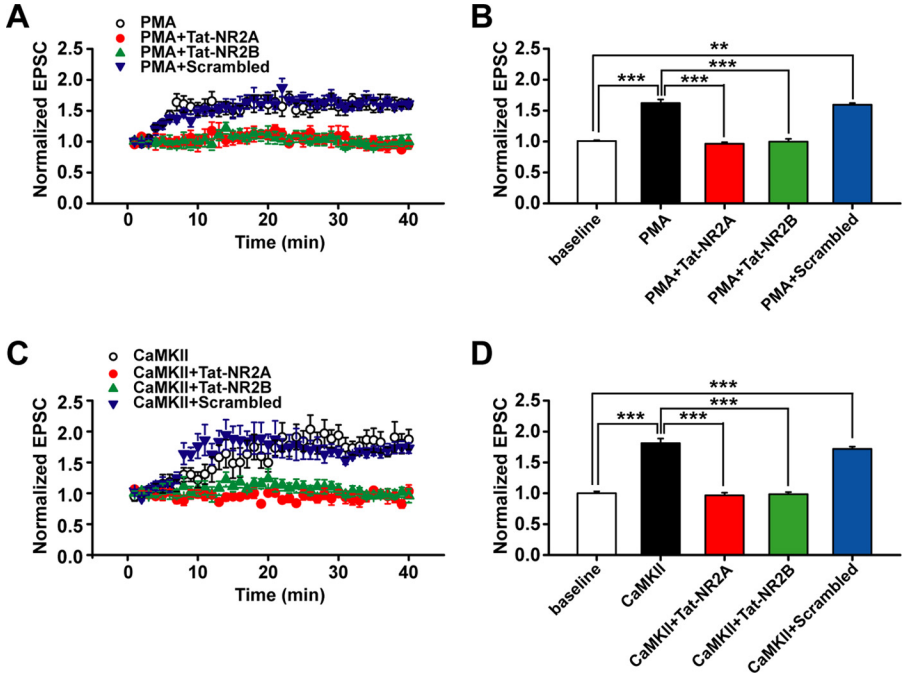

FIGURE 8. **Disturbing the association between NR2 subunits and CaMKII blocks LTP of AMPAR-mediated EPSCs induced by PKC or CaMKII.** *A*, PKC-induced chemical LTP of AMPAR-mediated EPSCs was abolished by interfering with the association of CaMKII with either NR2A or NR2B subunit. *B*, statistical plot of data displaying the effect of Tat-NR2A and Tat-NR2B as shown in *A*. *C*, similar findings for Tat-NR2A and Tat-NR2B were obtained on LTP induced by CaMKII activation. *D*, statistical plot of data displaying the effect of Tat-NR2A and Tat-NR2B as shown in *C*. The data of each group were obtained from four to six slices of three rats. **, $p < 0.01$; ***, $p < 0.001$ compared within the indicated groups; one-way ANOVA LSD test.

Our data provide new evidence for the hypothesis that PKC-dependent Src activation partially contributes to the potentiation of the activity of NMDA channels (8). Because most of the tyrosine kinase Src is located in the cell membrane, it is necessary for PKC to translocate to the cell surface to activate Src, which in turn phosphorylates NMDARs in the membrane. Thus, we determined whether PKC itself translocates to the postsynaptic membrane upon PKC activation. We detected a marked increase in the postsynaptic expression of PKC upon PKC activation (1.41 ± 0.04, $n = 4$, $p < 0.01$ compared with control) that was totally abolished by the PKC antagonist chelerythrine chloride (10 μM; 0.96 ± 0.10, $n = 4$, $p > 0.05$) but not by the CaMKII antagonist Myr-AIP (1.42 ± 0.11, $n = 4$, $p >$

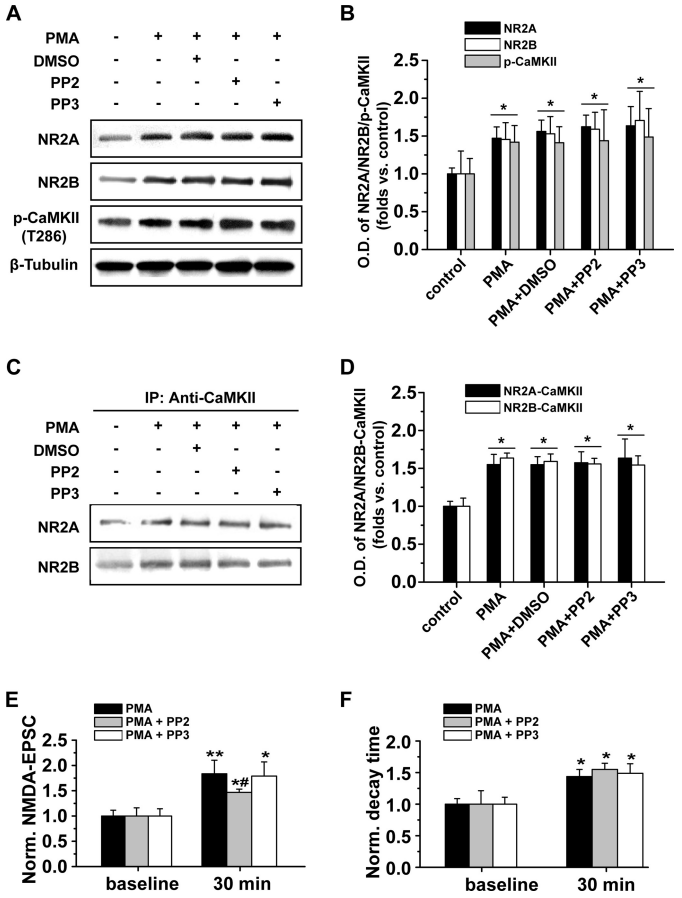

FIGURE 9. **Src signaling pathway is not required for PKC-induced NMDAR trafficking.** *A*, absence of changes in PKC-induced enhancement of postsynaptic expression of NMDAR NR2 subunits and CaMKII upon co-treatment with the Src antagonist PP2 (1 μM); its inactive analog, PP3 (1 μM); or vehicle DMSO and PMA (0.5 μM). *B*, statistical plot of data showing the absence of effect by Src antagonist as shown in *A*. *C*, co-IP assay revealed that the PKC-induced increased association between NR2 and CaMKII was unaffected by PP2 application. *D*, statistical plot showing similar results as in *C*. *E*, Src antagonist PP2 partially suppressed the enhancement of NMDA currents, whereas PP3 did not, supporting a role of Src family kinases in PKC-induced potentiation of NMDAR function through mechanisms other than those affecting NMDAR postsynaptic trafficking. *F*, absence of changes in decay time of NMDA current upon PP2 treatment, which might represent a proportional decrease in NR2A and NR2B components. *, $p < 0.05$ compared with control or base line; **, $p < 0.01$ compared with base line; #, $p < 0.05$ compared with PMA-treated group; one-way ANOVA LSD test. *Norm.*, normalized.

0.05; supplemental Fig. 5). These results support the interpretation that PKC trafficking is required for PKC-dependent Src activation and subsequent regulation of NMDA channel activity. This judgment receives support from previous *in vitro* biochemical investigations (44).

PKC and CaMKII Share Common Pathway in NMDA Regulation and LTP Induction—Previous investigations suggest a functional and positive cross-talk between PKC and CaMKII (12–15). However, the precise interaction between them is still uncertain. To test our hypothesis that PKC and CaMKII act in series and share at least a partial common pathway, we first checked how the LTP induced by PKC or CaMKII was affected by the activity of the other. Continuously perfusing slices with the selective CaMKII antagonist Myr-AIP (1 μM) completely abolished LTP induced by PMA (1.07 ± 0.02, $n = 5$, $p > 0.05$ compared with base line, paired-sample *t* test; Fig. 10*A1*). Similarly, application of the PKC-specific antagonist chelerythrine chloride (10 μM) completely blocked LTP induced by the active form of CaMKII (0.92 ± 0.02, $n = 5$, $p > 0.05$; Fig. 10*B1*). Treating slices with inactive CaMKII failed to induce LTP (supplemental Fig. 6). Interestingly, the concurrent changes in the amplitude and decay time of NMDA currents induced by PKC or CaMKII activation were also abolished by the antagonists targeting CaMKII and PKC, respectively (PMA + AIP/NMDA currents, 1.16 ± 0.08; $n = 10$; CaMKII + chelerythrine chloride/NMDA currents, 1.04 ± 0.10; $n = 7$; $p > 0.05$ compared with base line; Fig. 10, *A2* and *B2*). Combined with the data displayed in Fig. 8, these results suggest that alterations in NMDA EPSCs and in AMPAR-mediated LTP production induced by PKC or CaMKII are correlated, and each needs the activity of the other.

Using mutual occlusion experiments, we further investigated whether LTP induced by PKC and CaMKII share a common pathway. Perfusing slices with PMA (0.5 μM) for 15 min induced LTP (1.64 ± 0.02, $n = 5$, $p < 0.001$; supplemental Fig. 7). PMA at this concentration produced LTP with a saturated potentiation level (data not shown). When the potentiation level reached a stable plateau after 20 min, further CaMKII activation by loading recorded neurons with its active form through the recording pipette failed to produce additional potentiation ($p > 0.05$, paired-sample *t* test, $n = 6$; Fig. 10*C*). Similarly, after LTP was induced by CaMKII activation (1.61 ± 0.03, $n = 6$, $p < 0.001$, paired-sample *t* test; Fig. 10*D*), further PKC activation by PMA treatment failed to show additional potentiation ($p > 0.05$, paired-sample *t* test). These mutual occlusion experiments demonstrated that LTP induced by PKC and CaMKII activation uses a common cellular mechanism.

DISCUSSION

CaMKII Mediates PKC-induced NMDAR Trafficking—The insertion of NMDARs at the cell surface is tightly regulated in response to synaptic plasticity and sensory experience (4). The enhanced NMDAR insertion to postsynaptic sites, no matter whether it occurs along with increased AMPAR insertion or independently (19, 21, 45), may be a key step in regulating synaptic efficacy and remodeling. PKC promotes NMDAR trafficking independently of its phosphorylation of NMDARs and possibly through direct or indirect interaction with an NMDAR-associated protein (3). That PKC acts via Src family tyrosine kinases upon LTP induction in adult animals was proposed as a possible mechanism for the potentiated NMDAR trafficking (19). Our present study reveals that another NMDAR-associated protein kinase, CaMKII, which usually plays a central role in conventional NMDAR-dependent synaptic plasticity, is a key player in mediating PKC-induced enhancement of NMDAR trafficking. Using a combination of Western blot, immunofluorescence assay, co-IP, and whole-cell patch clamp recording, we demonstrated that PKC activation increased postsynaptic expression of autophosphorylated CaMKII and both NR2A and NR2B subunits. Further disturbing the association between NR2 subunits and CaMKII blocked the potentiation of NMDA trafficking induced by PKC activation, strongly suggesting that the enhancement and stability of the association between them, most possibly caused by

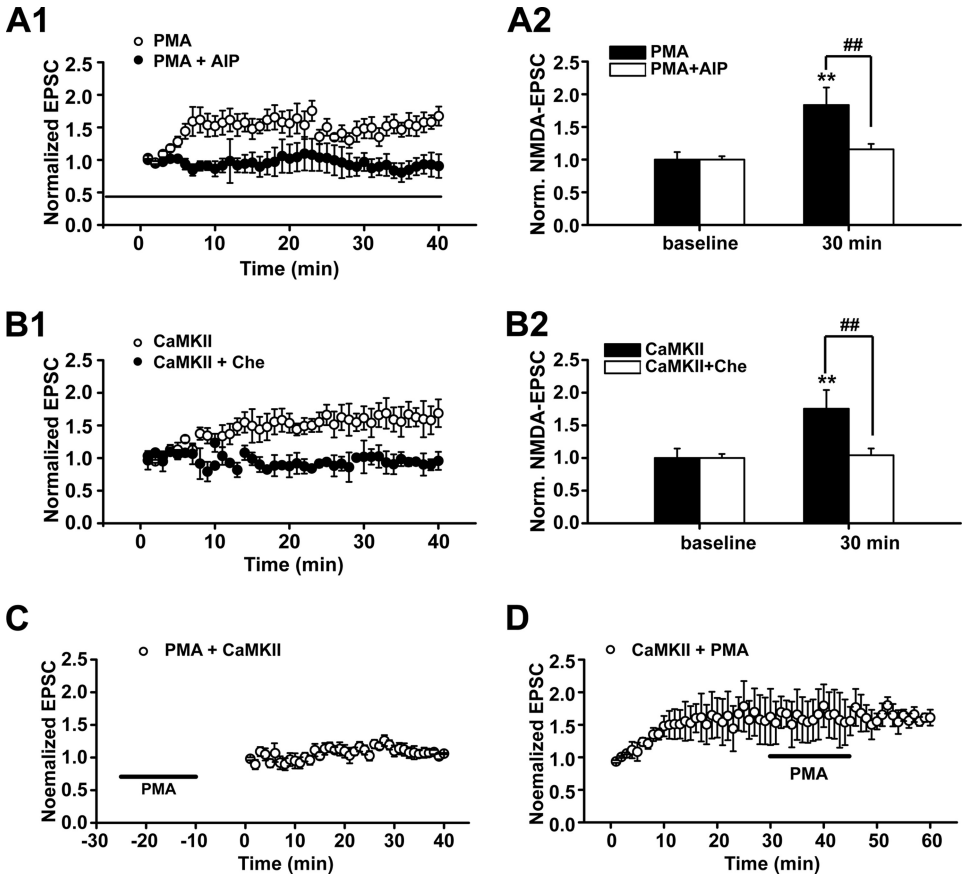

FIGURE 10. **PKC and CaMKII share common pathway in NMDA regulation and LTP induction of AMPAR-mediated EPSCs.** *A*, blocking CaMKII activity with Myr-AIP completely abolished both LTP (*A1*) and potentiation of NMDA currents (*A2*) induced by PKC activation. *B*, similar results were obtained when blocking PKC activity with chelerythrine chloride (*Che*; 10 μM) completely abolished LTP (*B1*) and potentiation of NMDA currents (*B2*) induced by CaMKII activation through loading recorded cells with active CaMKII (0.2 μM). *C* and *D*, mutual occlusion experiments revealed that PKC and CaMKII share a common pathway in LTP induction. *C*, CaMKII-induced LTP of AMPAR-mediated EPSCs was occluded by pretreating slices with PMA. Perfusing slices with PMA (0.5 μM) for 15 min induced LTP of AMPAR-mediated EPSCs (see supplemental Fig. 7). When the potentiation level reached a stable plateau 10 min later, further CaMKII activation by loading recorded neurons with active CaMKII through the recording pipette failed to produce additional potentiation. *D*, PMA-induced LTP of AMPAR-mediated EPSCs was occluded by preloading recorded cells with active CaMKII. Following LTP induced by CaMKII activation, further PKC activation by PMA treatment failed to show additional potentiation of AMPAR-mediated EPSCs. **, $p < 0.01$ compared with base line; ##, $p < 0.01$ compared with PMA-treated or active CaMKII-treated group; one-way ANOVA LSD test.

increased autophosphorylation of CaMKII, is critical for PKC-promoted trafficking.

Unexpected results came from the antagonistic effects of Tat-NR2A or Tat-NR2B on binding of both NR2A and NR2B subunits with CaMKII. However, considering that CaMKII phosphorylation upon PKC activation largely enhanced CaMKII-NR2B association and facilitated subsequent binding of NR2A with the identical CaMKII, a substantial portion of phosphorylated CaMKII was associated with both NR1/NR2A and NR1/NR2B, not to mention that almost one-third of NMDARs are in the form of NR1/NR2A/NR2B heterotrimers at the 2–3-week postnatal stage (46). To maintain the tight and stable association between NR1/NR2A/NR2B heterotrimers and CaMKII, the association between both NR2 subunits and CaMKII in the heterotrimers may be required. Therefore, disturbing either the NR2A- or NR2B-CaMKII binding would jeopardize the association of the other in binding to CaMKII and could cause its dissociation from the complex. However, by far, we could not totally exclude the possibility that other interacting proteins, such as L-type calcium channel, potassium channel, and ryanodine receptor, may bind to the same general location, causing either of the two Tat-NR2 peptides to affect association of CaMKII with both receptor subunits. Thus, the blockade by the peptides may not be a specific effect.

The present study demonstrates that increased NMDAR and CaMKII trafficking is accompanied by LTP production. Preventing NMDAR and CaMKII trafficking by either a peptide to disturb the NMDAR-CaMKII association or by a PKC antagonist abolished LTP induction. Although it was reported previously that activity-driven postsynaptic translocation of CaMKII has the potential to facilitate postsynaptic AMPA receptor accumulation as observed during LTP, these results might also suggest that the trafficking of NMDA receptors is correlated and required for AMPA receptor trafficking. This assumption receives support from one theoretical model that propose a structural role for CaMKII that links AMPA receptors via synapse-associated protein 97 (SAP97), band 4.1, F-actin, and actinin to NMDA receptors (47).

Our results point to the possibility that PKC and CaMKII act in series. CaMKII may be downstream of the PKC signaling pathway. PKC activation may indirectly activate CaMKII, possibly through triggering Src-dependent enhancement of NMDAR channel gating and the subsequent rapid increase in intracellular Ca^{2+} and Ca^{2+}/camodulin. Further mutual occlu-

sion experiments strengthen the conclusion that PKC and CaMKII share a common pathway at least in part. Taking into consideration that both PKC and CaMKII activate inositol 1,4,5-trisphosphate receptors or ryanodine receptors through direct phosphorylation (48), it is likely that PKC and CaMKII mutually activate each other by directly triggering intracellular Ca^{2+} release. Although one previous study reported that Thr-286 of CaMKII can be phosphorylated by PKC (49), no Ca^{2+}/calmodulin-independent activity or change in Ca^{2+}/camodulin-dependent activation was detected. Therefore, these results favor an indirect activation of CaMKII by PKC.

Possible Co-translocation of NR2 and CaMKII in Form of NR2-CaMKII Complex—Conventionally, CaMKII binding with NR2 subunits is thought to occur at postsynaptic sites. Upon NMDAR activation and subsequent extracellular Ca^{2+} influx, Ca^{2+}/camodulin binds and activates CaMKII, which triggers CaMKII autophosphorylation and subsequent translocation to postsynaptic sites where it binds directly to NMDARs (37, 47, 50). On the other hand, the NR2 subunit also translocates rapidly to postsynaptic sites upon LTP induction caused either by PKC activation or by typical paired stimulation (19, 20, 51). Thus, the retention of NR2 subunits in the cytoplasm after disturbing the NR2-CaMKII association could be explained by two major scenarios. First, CaMKII and NR2 subunits translocate independently to postsynaptic sites. Disturbing the NR2-CaMKII association causes p-CaMKII to dissociate from the NR2-CaMKII complex at the postsynaptic membrane and relocate to the cytoplasm. Due to the relatively lower Ca^{2+} levels in the cytoplasm and poor stability of p-CaMKII after dissociation from the complex, the p-CaMKII returns to the unphosphorylated form. The remaining NR2 subunits might also tend to be unstable and move from the postsynaptic membrane to the cytoplasm. However, this scenario seems unlikely, especially when taking into consideration the competition between CaMKII and PSD-95 for binding to the NR2A subunit of NMDARs (52). After dissociation from CaMKII, the NR2 subunits could be firmly anchored by binding to PSD-95 and retained at the postsynaptic membrane. Second, it is possible that upon PKC activation NR2 subunits first bind tightly with p-CaMKII, and then they are co-translocated to the postsynaptic membrane. Disturbing the NR2-CaMKII association antagonized the autophosphorylation of CaMKII and detained NR2 subunits in the cytoplasm. Our result that blocking the CaMKII phosphorylation with the antagonist Myr-AIP suppressed NR2 trafficking strongly supports this scenario but is against the first scenario.

Notably, our present results are at odds with some previous studies. First, one study has suggested that PKC activation inhibits binding between CaMKII and NR2A at postsynaptic sites (12). By contrast, our data support positive modulation of binding between CaMKII and NMDARs. This discrepancy could be due to the difference in the age of rats that were used in the two studies (18–21 days *versus* 2 months). Animals at an early developmental stage could display a substantially distinct mechanism underlying LTP-dependent events when compared with adult animals (19). A developmental shift could occur on PKC-dependent association of CaMKII and NR2 subunits. Second, it has been reported that PKC not only promotes postsynaptic translocation of CaMKII but also rapidly disperses NMDARs into the extrasynaptic domain (53) in contrast to our finding that PKC enhances expression of both NR2 subunits at postsynaptic sites. This inconsistency might be attributable to the different preparations used in the two studies (cultured cells *versus* acute brain slices). Our present results receive support from previous findings that PKC not only promotes surface expression of NMDARs but also enhances Src-dependent phosphorylation of postsynaptic NMDARs (3, 8, 54), which in turn facilitates the binding of phosphorylated NMDARs with a PSD protein such as PSD-95 and stabilizes the docking of postsynaptic NMDARs (9, 55).

Model for Differential Roles of CaMKII and Src in PKC-induced NMDA Potentiation—It has been reported that PKC-dependent activation of the non-receptor tyrosine kinase Src is at least partly responsible for the regulation of the activity of NMDA channels (8, 9). Src enhances NMDAR function mainly through potentiating NMDAR channel gating rather than regulating NMDAR trafficking (3, 8, 9, 11). Although one study shows that inhibition of endogenous Src activity prevents both the potentiation of NMDAR function and the decrease in intracellular NMDARs after LTP induction with tetanic stimulation in adult hippocampal slices (19), which suggests that Src is also required for LTP-associated NMDAR trafficking, no direct evidence was ever provided to support the Src-dependent regulation of postsynaptic NMDAR expression. Moreover, that study was performed on 6–8-week-old rats in which the mechanisms underlying NMDAR regulation and plasticity could be greatly different from those in younger, developing rats (19). Our study failed to detect any changes in postsynaptic NMDAR expression and in colocalization between NMDAR and CaMKII. Taking into consideration that both CaMKII and Src family enzymes are critical for LTP production as well as the fact that both are downstream molecules of the PKC signaling pathway, they might play distinct roles in PKC-induced potentiation of NMDAR function at temporally and spatially distinct stages. Our data on postsynaptic translocation of PKC itself after PKC activation match this speculation very well.

Based on previous findings as well as our present results, we propose a working model for regulation of NMDAR function accompanied by PKC-induced plasticity (supplemental Fig. 8). PKC activation first indirectly triggers CaMKII autophosphorylation and in turn markedly increases its association with NMDAR NR2 subunits followed by their co-trafficking to the postsynaptic membrane in the form of an NR2-CaMKII complex. Simultaneously, PKC is trafficked to postsynaptic sites where it activates Src family kinases and in turn mediates tyrosine phosphorylation of NMDARs. As a result, the gating of NMDAR channels is significantly enhanced. Therefore, CaMKII and Src independently and partly contribute to PKC-induced NMDAR potentiation through distinct mechanisms.

Acknowledgments—We thank Dr. Thomas R. Soderling for providing the active form of CaMKII and Dr. Luo Jian-Hong for providing the mouse anti-NR2B antibody. We also thank Dr. Gong Chen for constructive comments on the manuscript and Dr. Cui Lun-Biao for assistance with confocal imaging.

REFERENCES

1. Constantine-Paton, M., and Cline, H. T. (1998) *Curr. Opin. Neurobiol.* **8,** 139–148
2. Zoghbi, H. Y., Gage, F. H., and Choi, D. W. (2000) *Curr. Opin. Neurobiol.* **10,** 655–660
3. Lan, J. Y., Skeberdis, V. A., Jover, T., Grooms, S. Y., Lin, Y., Araneda, R. C., Zheng, X., Bennett, M. V., and Zukin, R. S. (2001) *Nat. Neurosci.* **4,** 382–390
4. Lau, C. G., and Zukin, R. S. (2007) *Nat. Rev. Neurosci.* **8,** 413–426
5. Zheng, X., Zhang, L., Wang, A. P., Bennett, M. V., and Zukin, R. S. (1999) *Proc. Natl. Acad. Sci. U.S.A.* **96,** 15262–15267
6. Lau, C. G., Takayasu, Y., Rodenas-Ruano, A., Paternain, A. V., Lerma, J., Bennett, M. V., and Zukin, R. S. (2010) *J. Neurosci.* **30,** 242–254
7. Suh, Y. H., Terashima, A., Petralia, R. S., Wenthold, R. J., Isaac, J. T., Roche, K. W., and Roche, P. A. (2010) *Nat. Neurosci.* **13,** 338–343
8. Lu, W. Y., Xiong, Z. G., Lei, S., Orser, B. A., Dudek, E., Browning, M. D., and MacDonald, J. F. (1999) *Nat. Neurosci.* **2,** 331–338
9. Salter, M. W., and Kalia, L. V. (2004) *Nat. Rev. Neurosci.* **5,** 317–328
10. Wang, Y. T., and Salter, M. W. (1994) *Nature* **369,** 233–235
11. Wang, Y. T., Yu, X. M., and Salter, M. W. (1996) *Proc. Natl. Acad. Sci. U.S.A.* **93,** 1721–1725
12. Gardoni, F., Bellone, C., Cattabeni, F., and Di Luca, M. (2001) *J. Biol. Chem.* **276,** 7609–7613
13. Malinow, R., Schulman, H., and Tsien, R. W. (1989) *Science* **245,** 862–866
14. Wang, J. H., and Feng, D. P. (1992) *Proc. Natl. Acad. Sci. U.S.A.* **89,** 2576–2580
15. Wang, J. H., and Kelly, P. T. (1995) *Neuron* **15,** 443–452
16. Gardoni, F., Schrama, L. H., van Dalen, J. J., Gispen, W. H., Cattabeni, F., and Di Luca, M. (1999) *FEBS Lett.* **456,** 394–398
17. Leonard, A. S., Lim, I. A., Hemsworth, D. E., Horne, M. C., and Hell, J. W. (1999) *Proc. Natl. Acad. Sci. U.S.A.* **96,** 3239–3244
18. Strack, S., and Colbran, R. J. (1998) *J. Biol. Chem.* **273,** 20689–20692
19. Grosshans, D. R., Clayton, D. A., Coultrap, S. J., and Browning, M. D. (2002) *Nat. Neurosci.* **5,** 27–33
20. Peng, Y., Zhao, J., Gu, Q. H., Chen, R. Q., Xu, Z., Yan, J. Z., Wang, S. H., Liu, S. Y., Chen, Z., and Lu, W. (2010) *Hippocampus* **20,** 646–658
21. Watt, A. J., Sjöström, P. J., Häusser, M., Nelson, S. B., and Turrigiano, G. G. (2004) *Nat. Neurosci.* **7,** 518–524
22. Barria, A., and Malinow, R. (2002) *Neuron* **35,** 345–353
23. Collingridge, G. L., Isaac, J. T., and Wang, Y. T. (2004) *Nat. Rev. Neurosci.* **5,** 952–962
24. Hayashi, T., Thomas, G. M., and Huganir, R. L. (2009) *Neuron* **64,** 213–226
25. Barria, A., and Malinow, R. (2005) *Neuron* **48,** 289–301
26. Arnold, D. B., and Clapham, D. E. (1999) *Neuron* **23,** 149–157
27. Kim, M. J., Futai, K., Jo, J., Hayashi, Y., Cho, K., and Sheng, M. (2007) *Neuron* **56,** 488–502
28. Zha, X. M., Dailey, M. E., and Green, S. H. (2009) *J. Neurosci. Res.* **87,** 1969–1979
29. Caputi, A., Gardoni, F., Cimino, M., Pastorino, L., Cattabeni, F., and Di Luca, M. (1999) *Eur. J. Neurosci.* **11,** 141–148
30. Zhao, M. G., Toyoda, H., Lee, Y. S., Wu, L. J., Ko, S. W., Zhang, X. H., Jia, Y., Shum, F., Xu, H., Li, B. M., Kaang, B. K., and Zhuo, M. (2005) *Neuron* **47,** 859–872
31. Mangels, L. A., and Gnegy, M. E. (1990) *Mol. Pharmacol.* **37,** 820–826
32. Osten, P., Khatri, L., Perez, J. L., Köhr, G., Giese, G., Daly, C., Schulz, T. W., Wensky, A., Lee, L. M., and Ziff, E. B. (2000) *Neuron* **27,** 313–325
33. Monyer, H., Burnashev, N., Laurie, D. J., Sakmann, B., and Seeburg, P. H. (1994) *Neuron* **12,** 529–540
34. Kang, N., Xu, J., Xu, Q., Nedergaard, M., and Kang, J. (2005) *J. Neurophysiol.* **94,** 4121–4130
35. Tojima, T., Akiyama, H., Itofusa, R., Li, Y., Katayama, H., Miyawaki, A., and Kamiguchi, H. (2007) *Nat. Neurosci.* **10,** 58–66
36. Colbran, R. J., and Brown, A. M. (2004) *Curr. Opin. Neurobiol.* **14,** 318–327
37. Merrill, M. A., Chen, Y., Strack, S., and Hell, J. W. (2005) *Trends Pharmacol. Sci.* **26,** 645–653
38. Strack, S., McNeill, R. B., and Colbran, R. J. (2000) *J. Biol. Chem.* **275,** 23798–23806
39. Hashida, H., Miyamoto, M., Cho, Y., Hida, Y., Kato, K., Kurokawa, T., Okushiba, S., Kondo, S., Dosaka-Akita, H., and Katoh, H. (2004) *Br. J. Cancer* **90,** 1252–1258
40. Cline, H. T., Debski, E. A., and Constantine-Paton, M. (1987) *Proc. Natl. Acad. Sci. U.S.A.* **84,** 4342–4345
41. Kleinschmidt, A., Bear, M. F., and Singer, W. (1987) *Science* **238,** 355–358
42. Morris, R. G., Anderson, E., Lynch, G. S., and Baudry, M. (1986) *Nature* **319,** 774–776
43. Yu, X. M., Askalan, R., Keil, G. J., 2nd, and Salter, M. W. (1997) *Science* **275,** 674–678
44. Akers, R. F., Lovinger, D. M., Colley, P. A., Linden, D. J., and Routtenberg, A. (1986) *Science* **231,** 587–589
45. Bashir, Z. I., Alford, S., Davies, S. N., Randall, A. D., and Collingridge, G. L. (1991) *Nature* **349,** 156–158
46. Al-Hallaq, R. A., Conrads, T. P., Veenstra, T. D., and Wenthold, R. J. (2007) *J. Neurosci.* **27,** 8334–8343
47. Lisman, J., Schulman, H., and Cline, H. (2002) *Nat. Rev. Neurosci.* **3,** 175–190
48. Bultynck, G., Vermassen, E., Szlufcik, K., De Smet, P., Fissore, R. A., Callewaert, G., Missiaen, L., De Smedt, H., and Parys, J. B. (2003) *Biochem. Biophys. Res. Commun.* **311,** 1181–1193
49. Waxham, M. N., and Aronowski, J. (1993) *Biochemistry* **32,** 2923–2930
50. Shen, K., and Meyer, T. (1999) *Science* **284,** 162–166
51. Bellone, C., and Nicoll, R. A. (2007) *Neuron* **55,** 779–785
52. Gardoni, F., Schrama, L. H., Kamal, A., Gispen, W. H., Cattabeni, F., and Di Luca, M. (2001) *J. Neurosci.* **21,** 1501–1509
53. Fong, D. K., Rao, A., Crump, F. T., and Craig, A. M. (2002) *J. Neurosci.* **22,** 2153–2164
54. Zheng, C. Y., Yang, X. J., Fu, Z. Y., and Luo, J. H. (2006) *Acta Pharmacol. Sin.* **27,** 1580–1585
55. Rong, Y., Lu, X., Bernard, A., Khrestchatisky, M., and Baudry, M. (2001) *J. Neurochem.* **79,** 382–390